REFINED SWISS AVALANCHE TERRAIN MAPPING CATv2 / ATHv2

Stephan Harvey[1]*, Marc Christen[2], Yves Bühler[1,3], Cyrill Hänni[1], Noel Boos[1], Boris Bernegger[1]

[1] *WSL Institute for Snow and Avalanche Research SLF, Davos, Switzerland*
[2] *RAMMS AG, Davos Wiesen, Switzerland*
[3] *Climate Change, Extremes and Natural Hazards in Alpine Regions Research Center CERC, Davos, Switzerland*

ABSTRACT: Avalanche terrain maps are becoming increasingly common for large areas due to the availability of high-resolution and high-quality digital elevation models (DEM). Many of these maps use the Avalanche Terrain Exposure Scale (ATES) classification system, which categorizes terrain from simple to extreme, often using simple runout models such as the statistical alpha-beta model to identify potential runout areas. The current automated ATES classification models do not include avalanche dynamics models such as RAMMS, SAMOS or r.avaflow. Since 2018, Classified Avalanche Terrain (CAT) and Avalanche Terrain Hazard (ATH) maps have been introduced in Switzerland, delineating avalanche terrain into potential release areas and runout zones for size class 3 avalanches determined with the numerical avalanche simulation model RAMMS. While these maps have been very well received by recreationists and are widely used in Switzerland, the experience gained over the last years has shown that there is still room for improvements. Specifically, (i) potential release areas were not always well classified, (ii) runout zones may be too long for typical skier-triggered avalanches, and (ii) the ATH map, combining various factors, is complex and the information can be ambiguous. Therefore, we present updated versions of the CAT and ATH maps addressing these issues and allowing users to better assess avalanche risk and plan backcountry trips. These revised maps provide refined representations of potential release areas and improved mapping of avalanche runout zones driven by a new version of RAMMS::EXTENDED. Validation in different regions, focusing on size 3 avalanches, confirm the improved accuracy in delineating potential avalanche runout zones. Additionally, a new iteration of the ATH map simplifies the complexity of avalanche terrain by categorizing the terrain into easy-to-understand classifications that provide a concise overview, which also incorporates the ATES system. The new maps are generated using various layers provided by the RAMMS output, which can also support automatic risk assessment at cruxes. All that is required to produce these new maps is a high-quality elevation model at 5-m resolution, and a reliable map layer for the protective forest cover.

KEYWORDS: avalanche terrain maps, white risk, avalanche terrain, avalanche hazard mapping, backcountry tour planning

1. INTRODUCTION

Terrain is a critical factor in assessing avalanche risk in the winter backcountry. It directly affects both the likelihood of avalanche release and the severity of its consequences. Key factors such as slope angle and curvature significantly influence the potential for avalanche release (Vontobel et al., 2013 and Stoffel et al., 2024). Furthermore, the characteristics of the entire avalanche path determine the consequences when caught in an avalanche. Consequently, selecting appropriate terrain under the given avalanche conditions is essential for backcountry travelers. To evaluate, describe, and communicate the complexities of avalanche terrain, Statham et al. (2006) introduced the Avalanche Terrain Exposure Scale (ATES). An updated version categorizing avalanche terrain from "simple" to "extreme" was recently presented (Statham et al., 2024). However, in this framework, terrain assessment relies heavily on expert judgement, sometimes leading to inconsistencies. As a result, recent developments have focused on automating terrain assessment to make it more objective.

Avalanche terrain maps, derived from high-quality Digital Elevation Models (DEM), are increasingly accessible on various tour planning platforms. These maps often incorporate automated implementations of the ATES system (e.g. Schmudlach and Köhler, 2016; Larson, 2020; Huber, 2023; Sykes, 2024; Toft, 2024). However, automated ATES maps typically depend on simplified runout models, such as the statistical alpha-beta model (Lied and Bakkehøi, 1980) or Flow-Py (D'Amboise et al., 2022), and do not integrate advanced avalanche dynamics

* *Corresponding author address:*
Stephan Harvey, WSL Institute for Snow and Avalanche Research SLF, Flüelastrasse 11, CH-7260 Davos Dorf, Switzerland,
phone: +41 81 417 01 29, fax: +41 81 417 01 10;
email: harvey@slf.ch

models like RAMMS (Christen et al., 2010), SAMOS (Sampl and Zwinger, 2004), or r.avaflow (Mergili, 2023).

An alternative approach, developed by Harvey et al. (2018), classifies avalanche terrain by delineating potential release areas and runout zones specifically for size class 3 avalanches. This method employs the RAMMS numerical avalanche simulation model (Christen et al., 2010) to generate Classified Avalanche Terrain (CAT) and Avalanche Terrain Hazard (ATH) maps. The CAT map clearly distinguishes between release areas and runout zones, while the ATH map offers a broader assessment of avalanche terrain hazards, including potential consequences, without explicitly separating release areas from runouts.

Since their introduction in Switzerland in 2018, these maps have been widely used. However, practical experience has highlighted areas for improvement. For example, the classification of potential release areas has not always been satisfactory, especially in extreme terrain, runout predictions for size class 3 avalanches have occasionally been too long regarding typical skier triggerd avalanche and the calculated potential consequences have been unsatisfactory on some cases. Additionally, the ATH map can sometimes be ambiguous because it combines various factors, such as trigger potential and consequences, and does not clearly distinguish between release area and runout zones. Furthermore, some simulations, based on 10-meter DEMs, which produced less precise results.

Our objective were therefore to refine the avalanche terrain maps to address these issues. We present an updated methodology aimed at enhancing the calculation of background layers used in creating the CAT and ATH maps. Furthermore, we explore the possibility of developing a simplified avalanche terrain hazard map (ATH) that distinguishes between release areas and runouts based on a refined ATES classification. This approach aims to propose a easy to understand and objective tool for evaluating avalanche terrain in the winter backcountry.

2. REFINED METHODOLOGY

The avalanche terrain maps CAT and ATH were created from several background layers (Harvey et al., 2018). Here we provide a brief description of the layers and the improvements we made.

2.1 *Potential release areas*

The potential for avalanche release was assessed using frequency statistics derived from multiple terrain features. To capture the frequency of combined terrain characteristics across more than 5,000 avalanche release areas in the region of Davos, we streamlined the terrain features originally reported by Harvey et al. (2018) from three to two key factors: slope angle and curvature. With these two features, we generated a two-dimensional density kernel estimate from all avalanche release areas. This density estimate allowed us to determine the probability of any given location being part of an avalanche release zone. Consequently, we developed a density layer, referred to as "layer 1," to quantify potential avalanche release areas (Fig. 1).

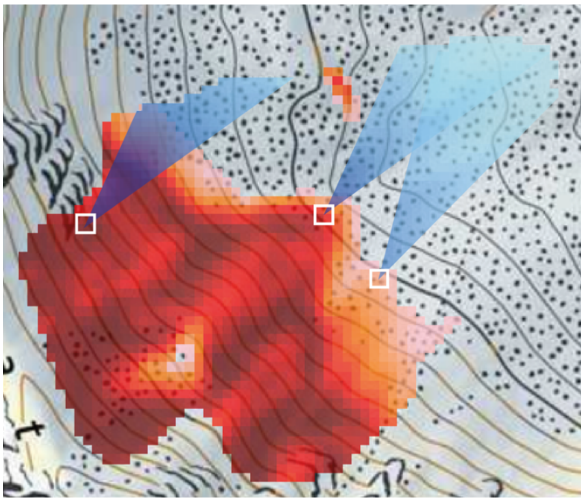

Figure. 1: Red shaded areas show how frequent the terrain features at a specific pixel is in comparison with avalanche release areas in the region of Davos (layer 1). The darker the red the more frequent the terrain. Blue shows the applied directional kernel calculation from tree example pixels to generate “layer2” – the triggering potential.

2.2 *Areas with increased remote triggering potential*

To identify areas with increased potential for remote triggering, we made only minor adjustments to the procedure used in the previous version. A directional Weibull kernel was generated using data from 75 remotely human-triggered avalanches (Harvey et al. 2018). This kernel was applied in the gradient direction, starting with the values from each pixel of "layer 1". Features that might inhibit crack propagation, such as forests, rough terrain, wide roads, or cliffs, were incorporated into the calculation by applying weighting factors. In contrast to the previous version, this method was capable to estimate the potential for triggering an avalanche across its entire extent (release area and runout), and to achieve a smooth transition from the release area to the zones below. The resulting raster was named "layer 2."

2.3 *Simulated avalanches*

The extent of potential size class 3 avalanches was calculated using an updated version of RAMMS::EXTENDED (e.g. Bartelt et al., 2012; Bartelt et al., 2016; Glaus et al., 2024). This new version includes enhancements to entrainment processes. The simulations not only determined the runout perimeter of the avalanches but also calculated several substantial parameters, such as deposition, velocity, and flow direction. These parameters were used to create consequence layers for potential deep burial or serious injury. Further counts of overlapping avalanche paths were used to quantify exposure which was used for the proposed classified ATHc map. To achieve more accurate and high-resolution results, we employed a 5-meter digital terrain model in the simulations. The release polygons were automatically predefined using an object-based approach as proposed by Bühler et al. (2013) and Bühler et al. (2018). Each polygon was used to determine a corresponding extent for running the simulation with specific input variables (e.g., a fracture depth of 0.6 m). For very small slopes (approx. <200 m^2) excluded from the RAMMS simulations, a simple slope gradient approach was applied.

2.4 *Potential consequences from burial*

The calculation of the potential burial begins with the deposition depth provided by RAMMS and the avalanche's flow direction. The snow amount in the deposit is then extrapolated upslope along this flowline. Flow accumulation is considered, giving greater weight to cells influenced by multiple flowlines. As a result, areas within the avalanche where the flowline leads to deep deposits are assigned a higher consequence value compared to those where the flowline leads to shallow deposits.

2.5 *Potential consequences for injury*

For each potential release pixel, flowlines were computed following the path of steepest descent. Along these lines, accelerations were derived from the simulated RAMMS velocities and further weighted when encountering cliffs or forests. The potential for serious injury from a pixel within the RAMMS simulation was then assessed by summing the weighted downward accelerations. A threshold was established, above which fatal injuries were considered likely.

3. RESULTS

The above-mentioned adjustments led to the following results, which were compared with the 2018 version (Harvey et al., 2018).

3.1 *Improved classified potential release areas*

The calculations using the 2D density kernel are not only easier to understand but also produce more accurate results. In particular, more rough terrain with slopes close to or higher than 40° are classified more effectively in the new version compared to the older one (Fig. 2).

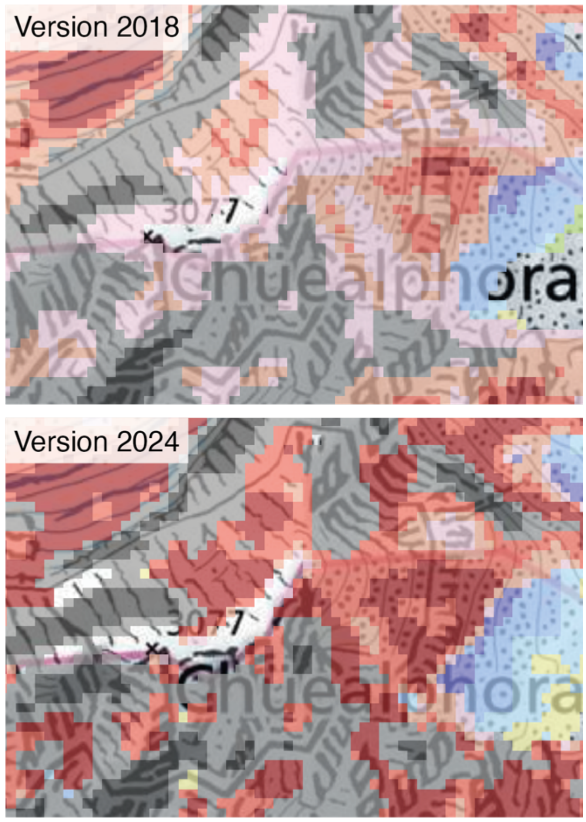

Figure 2: Comparison of classified potential release areas (red color) between the 2018 version (top) and the new version (bottom). The darker the red the more likely a release area. The new approach more accurately classifies terrain, particularly slopes 40° or steeper.

3.2 *Improved avalanche runout from RAMMS*

The simulated avalanche extents were compared with a dataset of 5000 observed maximum size class 3 avalanches as well as with a dataset of about 300 human triggered avalanches both in the region of Davos. From the lowest point of each avalanche flowlines were generated in the direction of the steepest gradient slope downward if the point was within the RAMMS simulation, otherwise slope upward. From each flowline the distance from either leaving or entering the simulated area was calculated. The results in Figure 3 show that for both data sets the simulations got closer to the lowest point of the avalanche. The percentage of depots exceeding the simulated perimeter did not change.

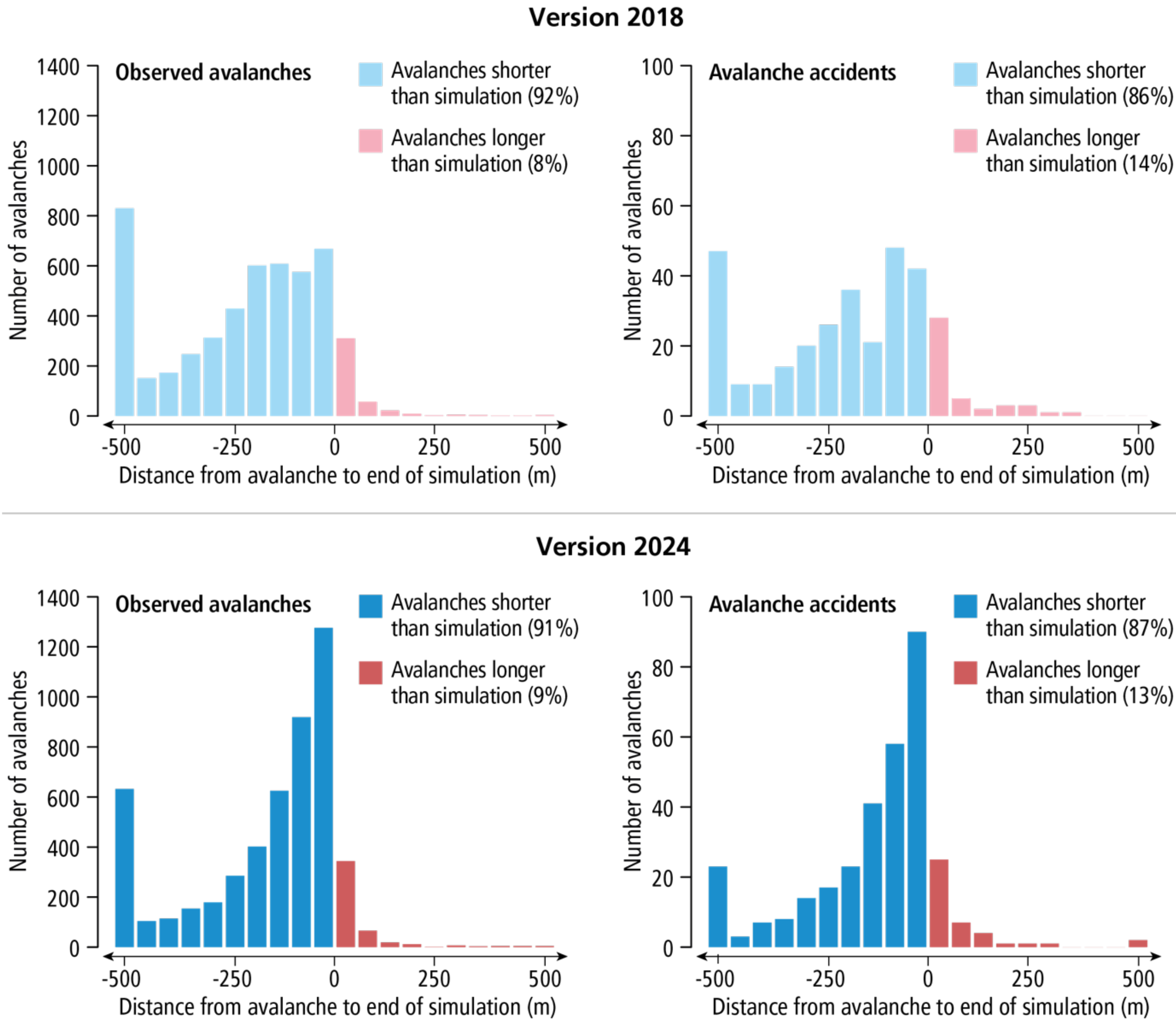

Figure 3: Comparison of distances between the lowest points of approx. 5,000 observed size 3 avalanches (left) and 300 human-triggered accidental avalanche (right) with RAMMS-simulated extents. The upper graphs show the 2018 version results, while the lower graphs present the updated version. Blue bars indicate avalanches shorter than the simulations; red bars indicate those that exceeded the simulated extents. In general the distance between the lowest point of the avalanches to the end of the sumulated runout has decreased from the version of 2018 to the one of 2024.

3.3 <u>Consequences on the basis of RAMMS outputs</u>

An example of the calculated potential for deep burial and for serious injuries in case of an avalanche is shown in Figure 4.

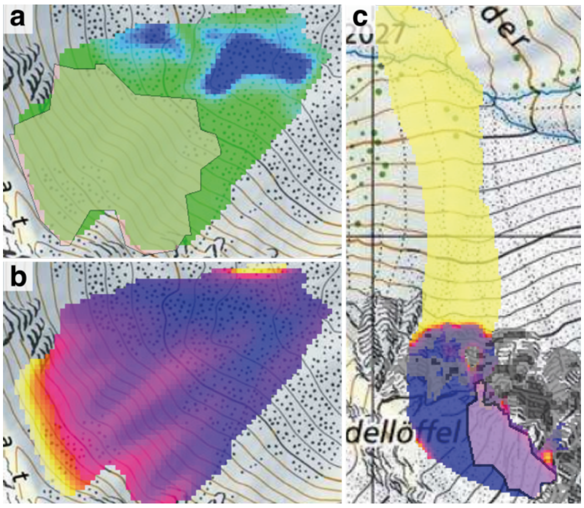

Figure 4. Examples of two RAMMS simulations from a given release polygon. The lower left (b) shows the deep burial potential calculated from the deposit (a), while the right (c) highlights the potential of serious injury from a cliff fall. Dark violet shading in (b) and (c) indicates severe consequences.

3.4 *Included avalanche simulations in forest*

The forest significantly influences avalanche terrain. It can both reduce or prevent an avalanche from releasing and slow down its movement. In contrast to the 2018 version, the updated map now highlights the run-out area of a simulated avalanche within the forested region (Fig. 5). This area is marked in light green, making it stand out from the surrounding forest, which is represented as either forested or non-forested.

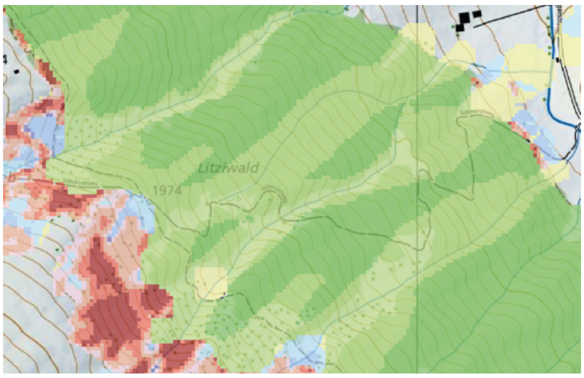

Figure 5. Example of RAMMS simulations showing avalanche flow into a forest. Light green shading indicates the intersection between the forest and the avalanche runout.

4. NEW AVALANCHE TERRAIN MAPS

By combining the layers described in section 2, the final map layers were produced (Fig. 6). In addition to the well-known CAT and ATH maps, we also introduce a simplified map that closely aligns with the ATES classification. This new map layer represents an advanced and more easily interpretable version of the ATH map layer.

4.1 *Updated CAT and ATH map layers*

The existing CAT and ATH map layers were updated using the refined methodologies. The new version of the classified avalanche terrain (CAT) map was created by combining the following background layers: (a) potential avalanche release, (b) remote triggering potential, and (c) the extent of the RAMMS simulations (Fig. 6).

The updated avalanche terrain hazard (ATH) map incorporates the same RAMMS simulation extent but combines the CAT map's release and trigger potential with the potential consequences of being caught in an avalanche, such as deep burial or serious injury. However, the same colors on the map can arise from different factors, leading to ambiguous and unclear map interpretations. To address this, we created a simplified, more user-friendly version of the ATH map based on the ATES rating system (ATHc).

4.2 *Proposed classified ATH map based on ATES rating*

The ATES rating system for describing avalanche terrain is based on criteria such as avalanche release, consequences and exposure (Statham et al., 2024). These criteria can be derived from the ATH map layer and from the RAMMS simulations. The ATH map incorporates terrain with regard to potential avalanche release, avalanche triggering and the potential consequences in case of being caught by an avalanche. An estimate of the exposure can be derive by counting overlapping RAMMS simulations of the different avalanche sizes.

Using the results of the ATH map and an exposure layer derived from the RAMMS simulations (Fig. 6), we initially classified the terrain into the ATESv2 ratings: 'simple,' 'challenging,' 'complex,' and 'extreme.' Like the ATH maps, this classification does not distinguish between potential release areas, avalanche paths, or runout zones. To address this, we introduced two subclasses in the second step: 'challenging release' within the 'challenging' category and 'complex runout' within the 'complex' category. This refines the ATES classification by clearly distinguishing between release and runout areas (Table 1). The resulting classified terrain hazard map has been designated as 'ATHc' (Fig. 6).

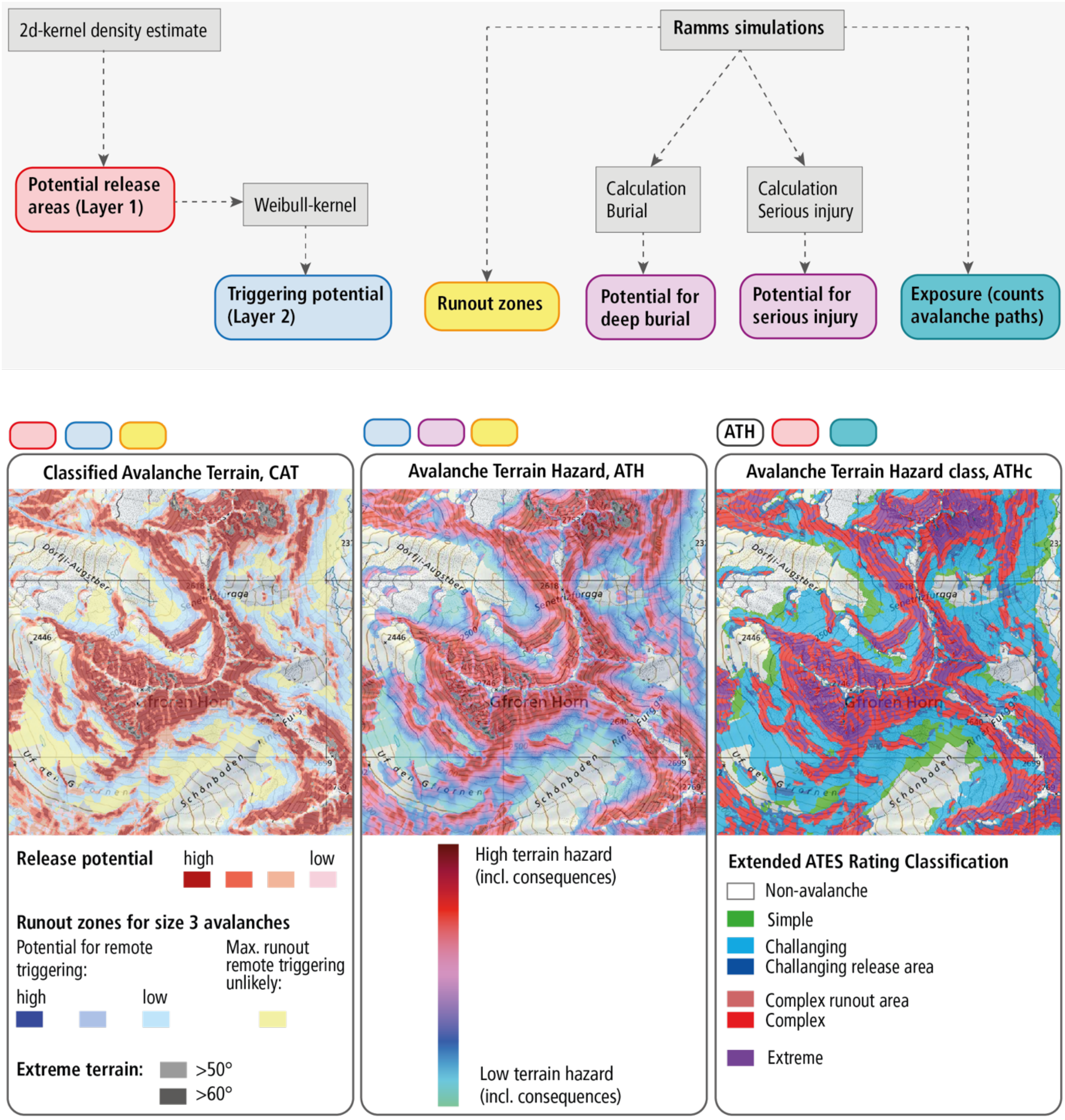

Figure 6: Overview of the map creation process. The top section presents a brief workflow for deriving the background layers, shown in colored boxes. Below, the three resulting map layers are shown. The colored boxes above each map indicate which layers were used in its creation.

Table 1: Extended ATES rating distinguishing between potential release areas and avalanche runout zones. This rating was used to develop the simplified avalanche terrain map, ATHc.

Class (extended ATES rating)	**Runout (<30°)**	**Pot. release area (≥30°)**
simple	x	
challenging	x	
challenging release		x
complex runout	x	
complex		x
extreme		x

5. DISCUSSION

We presented an updated version of the CAT and ATH avalanche terrain maps, incorporating several key improvements. The classification of potential avalanche release areas has been enhanced, particularly on slopes with gradients around 40°. Additionally, the RAMMS simulations were improved, which had an effect the layers derived from it. For the RAMMS simulation we now used a 5m DEM, compared to the 10m DEM in the previous version. While this adjustment increased calculation times, it yielded more accurate results. A comparison with two different avalanche datasets shows that the new simulations more closely match observed avalanches, compared to the earlier version. Furthermore, the assessment of consequences in case of being caught by an avalanche now incorporates RAMMS-simulated depositions to estimate the potential for deep burials, as well as velocity and accelerations to evaluate the potential for serious injury.

The updated avalanche terrain maps are built on multiple layers, enabling the evaluation of various criteria from the ATESv2 technical model (Statham et al., 2024). We propose a new simplified ATH map (ATHc), which includes an ATES classification based on an automated overall evaluation of the ATESv2 rating. To differentiate between potential release areas and runout zones, we further subdivided the "challenging" and "complex" classifications into "challenging release" and "complex runout", respectively. Consequently, potential avalanche release areas are now classified as "extreme," "complex," or "challenging release," while potential runout zones are categorized as "simple," "challenging," or "complex runout" (Table 1). The new ATHc map layer integrates all critical aspects of avalanche terrain and could serve as a valuable tool for beginners planning backcountry tours.

6. CONCLUSIONS AND OUTLOOK

Although the updated avalanche terrain maps show significant improvements, it is important to note that the simulations are focused on size class 3 avalanches. In avalanche cycles involving very large or extreme avalanches, even areas not classified as avalanche terrain can be affected. This means that the proposed avalanche terrain maps must be interpreted with caution in very critical avalanche situations, typically in forecasted “high” avalanche danger. Further, the simplified representation of forests as either forested or non-forested may lead to inaccurate results. Rapid changes in glaciated areas may also cause discrepancies between simulated and actual slope features.

The CAT and ATH maps are available on the White Risk platform (whiterisk.ch). The outcome of the various layers is further used for automatic crux detection and assessment (Harvey et al, 2023 and 2024). Following a test phase, we plan to release the new ATHc map as well.

Looking ahead, we can now readily determine these updated maps to other mountain regions worldwide, provided that accurate DEM and forest data are available.

ACKNOWLEDGEMENT

We thank Marc Bitterli for the improvements on simulating the consequences and Marcel Puschnig for technical support.

Many thanks to Andreas Stoffel for GIS support, Perry Bartelt for better understanding the RAMMS simulations.

Many thanks to all practitioners and White Risk users, who gave substantial input.

Finally, we would like to thank Alec van Herwijnen for reviewing this article.

REFERENCES

Bartelt, P., Christen, M., Bühler, Y., Caviezel, A. and Buser, O., 2018. Snow entrainment: Avalanche interaction with an erodible substrate, Proceedings ISSW 2018. International Snow Science Workshop, Innsbruck, Austria, 7-12 October 2018.

Bartelt, P., Buser, O., Vera Valero, C. and Bühler, Y., 2016. Configurational energy and the formation of mixed flowing/powder snow and ice avalanches. Ann. Glaciol., 57(71): 179-188.

Bühler, Y.; Bebi, P.; Christen, M.; Margreth, S.; Stoffel, L.; Stoffel, A.; Marty, C.; Schmucki, G.; Caviezel, A.; Kühne, R.; Wohlwend, S.; Bartelt, P., 2022: Automated avalanche hazard indication mapping on a statewide scale. Natural Hazards and Earth System Sciences, 22, 6: 1825-1843. https://doi.org/10.5194/nhess-22-1825-2022

Bühler, Y., von Rickenbach, D., Stoffel, A., Margreth, S., Stoffel, L., Christen, M., 2018. Automated snow avalanche release area delineation - validation of existing algorithms and proposition of a new object-based approach for large scale hazard indication mapping, Natural Hazards and Earth System Science Discussion, https://doi.org/10.5194/nhess-2018-124.

Bühler, Y., Kumar, S., Veitinger, J., Christen, M., and Stoffel, A.: Automated identification of potential snow avalanche release areas based on digital elevation models, Natural Hazards and Earth System Sciences, 13, 1321-1335, https://doi.org/10.5194/nhess-13-1321-2013, 2013.

Christen, M., Kowalski, J., and Bartelt, P., 2010. RAMMS: Numerical simulation of dense snow avalanches in three-dimensional terrain, Cold Reg. Sci. Technol., 63, 1-14.

D'Amboise, C. J. L., Neuhauser, M., Teich, M., Huber, A., Kofler, A., Perzl, F., Fromm, R., Kleemayr, K., and Fischer, J. T.: Flow-Py v1.0: A customizable, open-source simulation tool to estimate runout and intensity of gravitational mass flows, Geoscientific Model Development, 15, 2423-2439, https://doi.org/10.5194/gmd-15-2423-2022, 2022.

Delparte, D, Jamieson, B and Waters, N. 2008. Statistical runout modeling of snow avalanches using GIS in glacier national park, Canada. Cold Regions Science and Technology 54, 183–192.

Glaus, J., Wikstrom Jones, K., Bartelt, P., Christen, M., Stoffel, L., Gaume, J., and Bühler, Y.: Simulation of cold powder avalanches considering daily snowpack and weather situations to enhance road safety, EGUsphere, 2024, 1-31, https://doi.org/10.5194/egusphere-2024-771, 2024.

Harvey, S., Nigg, P., 2009. Practical risk assessment and decision making in avalanche terrain. An overview of concepts and tools in Switzerland. In: Proceedings ISSW 2009. International Snow Science Workshop, 27 September - 2 October 2009, Davos, Switzerland, pp. 654-658.

Harvey, S.; Schmudlach, G.; Bühler, Y.; Dürr, L.; Stoffel, A.; Christen, M., 2018: Avalanche terrain maps for backcountry skiing in Switzerland. In: Proceedings ISSW 2018. International Snow Science Workshop, Innsbruck, Austria, 7-12 October 2018, pp. 1625-1631.

Harvey, S., Hänni, C., Boos, N., Urner, J. 2023. Automatic crux detection for planning backcountry tours in avalanche terrain. In: International snow science workshop proceedings 2023 (pp. 606 – 611)

Huber, A., Hesselbach, C., Oesterle, F., Neuhauser, M., Adams, M., Plörer, M., Stephan, L., Toft, H.B., Sykes, J., Mitterer, C., Fischer, J.T.: AutoATES Austria - Testing and Application of an Automated Model-Chain for Avalanche Terrain Classification in the Austrian Alps, in: Proceedings International Snow Science Workshop, Bend, OR, USA, 8-13 October 2023, 929-936.

Lied, K and Bakkehøi, S (1980) Empirical calculations of snow-avalanche run-out distance based on topographic parameters. Journal of Glaciology V26, 165–178.

Mergili, M.: Simulation of geomorphic mass flows: recent advances of the open-source simulation framework r.avaflow, 84th EAGE Annual Conference and Exhibition, 3364-3366, 2023

Oller P, Baeza C, Furdada G. Empirical α–β runout modelling of snow avalanches in the Catalan Pyrenees. Journal of Glaciology. 2021;67(266):1043-1054. https://doi.org/10.1017/jog.2021.50

Sampl P, Zwinger T. Avalanche simulation with SAMOS. Annals of Glaciology. 2004;38:393-398. https://doi.org/10.3189/172756404781814780

Schmudlach, G. and Köhler, J.: Method for an Automated Avalanche Terrain Classification, in: Proceedings International Snow Science Workshop, Breckenridge, USA, 729-736,

Statham, G. and Campbell, C. 2024. The Avalanche Terrain Exposure Scale (ATES) v.2. Nat. Hazards Earth Syst. Sci. Discuss. [preprint], https://doi.org/10.5194/nhess-2024-89, in review, 2024

Stoffel, A., Harvey, S., Bühler, Y. On the influence of snow depth on surface shape and roughness in the release areas of observed skier-triggered avalanches. In: International snow science workshop proceedings 2024

Sykes, J., Toft, H., Haegeli, P., and Statham, G.: Automated Avalanche Terrain Exposure Scale (ATES) mapping – local validation and optimization in western Canada, Nat Hazard Earth Sys, 24, 947-971, https://doi.org/10.5194/nhess-24-947-2024, 2024.

Toft, H. B., Sykes, J., Schauer, A., Hendrikx, J., and Hetland, A.: AutoATES v2.0: Automated Avalanche Terrain Exposure Scale mapping, Nat. Hazards Earth Sys, 24, 1779–1793, https://doi.org/10.5194/nhess-24-1779-2024, 2024.

Vontobel, I., Harvey, S. and Purves, R.S., 2013. Terrain analysis of skier-triggered avalanche starting zones. In: F. Naaim-Bouvet, Y. Durand and R. Lambert (Editors), Proceedings ISSW 2013. Inter-national Snow Science Workshop, Grenoble, France, 7-11 October 2013. ANENA, IRSTEA, Météo-France, Grenoble, France, pp. 371-375.